

Published in final edited form as:

Microbes Infect. 2011 September ; 13(10): 871–879. doi:10.1016/j.micinf.2011.04.011.

***Bordetella avium* Causes Induction of Apoptosis and Nitric Oxide Synthase in Turkey Tracheal Explant Cultures**

David M. Miyamoto¹, Kristin Ruff², Nathan M. Beach², Angella Dorsey-Oresto¹, Isaac Masters², and Louise M. Temple²

¹Department of Biology Drew University, Madison, NJ, 07940

²Department of Integrated Science and Technology, James Madison University, VA, 22801

Abstract

Bordetellosis is an upper respiratory disease of turkeys caused by *Bordetella avium* in which the bacteria attach specifically to ciliated respiratory epithelial cells. Little is known about the mechanisms of pathogenesis of this disease, which has a negative impact in the commercial turkey industry. In this study, we produced a novel explant organ culture system that was able to successfully reproduce pathogenesis of *B. avium* *in vitro*, using tracheal tissue derived from 26 day-old turkey embryos. Treatment of the explants with whole cells of *B. avium* virulent strain 197n and culture supernatant, but not lipopolysaccharide (LPS) or tracheal cytotoxin (TCT), specifically induced apoptosis in ciliated cells, as shown by annexin V and TUNEL staining. LPS and TCT are known virulence factors of *B. pertussis*, the causative agent of whooping cough. Treatment with whole cells of *B. avium* and LPS specifically induced NO response in ciliated cells, shown by uNOS staining and diaphorase activity. The explant system is being used as a model to elucidate specific molecules responsible for the symptoms of bordetellosis.

1. Introduction

Bordetellosis is an upper respiratory disease of turkeys caused by *Bordetella avium* in which pathogenic changes are triggered by bacterial attachment to ciliated respiratory epithelial cells [1]. Bordetellosis in birds is clinically characterized by sneezing, excessive ocular and nasal discharges, and labored breathing [2–3]. Ciliated cells are extruded from the epithelium and hyperplasia results in a respiratory epithelium composed of immature cells. Mucus is depleted, and there is eventual infiltration by lymphocytes and macrophages [2], [4]. In more serious cases of the disease, the tracheal rings become highly distorted resulting in a collapse of the trachea [2–3]. Similar pathogenic changes occur *in vitro* with turkey tracheal organ cultures [5–6], and are also seen during infection of *B. bronchiseptica* [7] and *B. pertussis* [8–11] in similar organ culture systems.

In response to *B. avium* infection and prior to extrusion, the ciliated cells exhibit blebbing, swelling, and cytoplasmic vacuolation [5], behaviors that suggest programmed cell death (apoptosis). Given the highly specific attachment of this bacterium to the ciliated cells, sloughing of infected cells is an effective measure to limit further invasion of the epithelia by the bacteria [12]. A number of toxins produced by other species of bacteria have been

© 2011 Elsevier Masson SAS. All rights reserved.

Publisher's Disclaimer: This is a PDF file of an unedited manuscript that has been accepted for publication. As a service to our customers we are providing this early version of the manuscript. The manuscript will undergo copyediting, typesetting, and review of the resulting proof before it is published in its final citable form. Please note that during the production process errors may be discovered which could affect the content, and all legal disclaimers that apply to the journal pertain.

shown to induce apoptosis by forming membrane pores, inhibiting protein synthesis, interfering with host cell signal transduction pathways, or triggering immune cell responses [13].

Another defensive response to bacterial and viral pathogens is the production of nitric oxide (NO,[14]). NO has been implicated as the main culprit in destruction of ciliated epithelial cells by *Bordetella pertussis* [15–18]. Intact bacteria as well as *B. pertussis* tracheal cytotoxin (TCT) and lipopolysaccharide (LPS) induce pathological changes mediated by NO [15–18]. Experimental suppression of induced nitric oxide synthase (iNOS) activity, either by corticosteroid treatment or by gene knockout, lowers effective immune responses to pathogens, including *B. pertussis* [19]. While NO has non-specific destructive potential due to the direct effects of nitrative and oxidative stress [20], it can also act as an intracellular messenger that either induces or blocks apoptosis depending on the cell type [21–22].

Nitric oxide synthase (NOS) is the enzyme that facilitates the NO response, and there are three isoforms that are produced in ciliated tracheal epithelial cells. Two of the isoforms, neuronal (nNOS) and endothelial (eNOS) nitric oxide synthases, are constitutive enzymes regulated by calmoduline and calcium. These constitutive isoforms produce NO that stimulates guanylate cyclase to make cGMP [14]. In the respiratory system the constitutive isoforms control bronchodilation and vasodilation [14] as well as ciliary beating [23]. In contrast, the third isoform, inducible nitric oxide synthase (iNOS) is regulated by transcriptional mechanisms. Consequently the production of NO by iNOS requires several hours, the quantities of NO produced are substantial, and NO production may be sustained for hours or days [14]. NO produced by iNOS is thought to play a role in non-specific defense against pathogens by forming reactive nitrogen radicals, eliciting T-cell responses, and promoting airway inflammation [14].

While *B. pertussis* and *B. bronchiseptica* cause similar pathological changes in ciliated respiratory cells, there are several toxins characterized in *B. pertussis* that have no obvious homologs in *B. avium* [24]. This leads to the question of whether the mechanisms and pathways that lead to cell destruction are the same in different *Bordetella* species. Consequently, a novel turkey trachea organ explant culture system was developed and used to examine the *in vitro* response of ciliated tracheal epithelial cells from the natural host, the domestic turkey, to *B. avium* infection with multiple cytochemical and immunochemical procedures that assess apoptosis and NO response. This model permits the study of the pathways leading to bordetellosis and allows for comparison of pathogenesis of *B. avium* with other *Bordetella* species.

2. Materials and Methods

2.1 Strains, bacterial proteins and culture conditions

The wild type strain 197n of *B. avium*, a clinical isolate that is virulent in turkey poults [1] was grown on Bordet-Gengou agar plates with 15% sheep blood the day before use. A 0.5 OD₆₀₀ suspension of bacteria was prepared in Earle's Balanced Salts Solution (EBSS) and diluted 1:10 to give a final concentration of approximately 10⁸ bacteria ml⁻¹. *B. pertussis* strain Tohama (gift of A. Weiss, University of Cincinnati), *B. bronchiseptica* strain RB50 (gift of J. Miller, UCLA), and *B. hinzii* SV2 (isolated from commercial turkeys in the Shenandoah Valley in 2007) were prepared identically to the *B. avium* strain. *B. bronchiseptica* lipopolysaccharide (LPS; gift from Andrew Preston, University of Bristol, UK) was resuspended in endotoxin-free H₂O and used at 1 and 10 µg ml⁻¹. *B. avium* 197N LPS was prepared and used at 10 µg ml⁻¹ as described by [25]. *B. pertussis* tracheal cytotoxin (TCT; gift from William Goldman, Washington University, St. Louis, MO) was resuspended in endotoxin-free H₂O and used at 1 µM. *B. pertussis* TCT is identical to TCT

produced by *B. avium* [26]. Secreted molecules were collected by growing *B. avium* on solid minimal media (CDM agar plates [27]) for 10 h. The bacteria and secreted materials were then scraped from the plate into EBSS, dispersed by briefly vortexing for 30 sec, concentration adjusted to an approximate 1.0 OD₆₀₀, and bacteria removed by pelleting at 3000 g for 10 min. The supernatants were then sterilized by passing through a 0.22 µm filter and diluted 1/10 in EBSS before use. This procedure minimizes the number of dead and broken cells during the preparation of molecules secreted by the bacteria. This secreted fraction was further divided coarsely into 3 molecular weight categories by gas-pressured filtration through Amicon filters with molecular weight cutoffs of 30 and 100 kDa.

2.2 Preparation of explant cultures

Trypsinized suspensions of tracheal epithelial cells formed ciliated cell aggregates whose constant motion precluded attachment. Consequently a tracheal explant procedure was developed. Collagen solution (Vitrogen collagen solution, Angiotech BioMaterials Corp., Palo Alto, CA.) was polymerized onto 22 mm square poly-lysine coated coverglasses and placed in 6 well tissue culture plates. Thin cross sections containing 2–3 cartilage rings were cut from the tracheas of 26 day-old embryonated Hybrid turkey eggs (British United Turkeys of America, Lewisburg, WV, and Ag-Forte Hatchery, Harrisonburg, VA). Four to eight tracheal rings were placed on each collagen-coated coverglass slip with a minimal amount of EBSS, incubated for 1 h at 37 °C to allow the rings to attach, and incubated in Media 199 containing 5% fetal calf serum and 1% antibiotic-antimycotic (~5,000 units penicillin, 5 mg streptomycin and 10 mg neomycin ml⁻¹, Sigma-Aldrich) for at least 4 days to allow the ciliated epithelia to grow out, forming a monolayer, on the collagen gel. Cultures were inspected for ciliary activity and rinsed of all debris and dead cells with EBSS prior to inoculation with the bacterial and other suspensions. Control cultures were incubated in EBSS while experimental cultures were incubated with bacteria for the times indicated. At the end of incubation, they were immediately treated and examined while still alive or fixed with 4% paraformaldehyde in phosphate buffered saline (PBS; pH 7.4) for 15 min to 1 h at room temperature, rinsed twice with PBS, and stored in PBS at 4 °C.

2.3 Apoptosis Induction Assays

2.3.1 Annexin V staining—During apoptosis membrane lipids are flipped from the cytoplasmic to the extracellular side of the membrane. Phosphatidylserine, which is normally only found on the cytoplasmic side of the membrane, now appears on the outside layer of the cell membrane [28]. Annexin V is a human anticoagulant protein with high binding affinity for phosphatidylserine and has been developed as an assay for apoptosis in commercially available kits ([29] Vybrant® Apoptosis Assay Kit #2, Invitrogen # V13241). Unfixed explant cultures were rinsed twice in cold PBS (pH 7.4; 5 min) and incubated in 200 µl of annexin-binding buffer (10 mM HEPES, 140 mM NaCl, and 2.5 mM CaCl₂, pH 7.4) containing 10 µl Annexin V Alexa Fluor-488 conjugate and 5 µl propidium iodide (PI), 1 mg ml⁻¹, for 15 min at room temperature in the dark. Cells were washed twice in annexin-binding buffer and analyzed by fluorescence microscopy. Cells were still alive and the beating of cilia could be observed and recorded by digital video recording. Using this commercially available kit, healthy, non-apoptotic cells show little or no annexin V staining, apoptotic cells show annexin V staining, while necrotic cells show both annexin V and PI staining.

2.3.2 TUNEL staining—Another sign of apoptosis is the fragmentation of DNA [30]. Broken ends of the DNA can be detected by using a terminal transferase dUTP nick end labeling (TUNEL) kit (DeadEnd™ TUNEL colorimetric kit, Promega #G7130). Fixed explants were permeabilized in 0.2% Triton® X-100 (Sigma-Aldrich) in PBS (5 min) and washed with plain PBS. Coverslips (with the explant facing up) were incubated with 200 µl

of recombinant terminal deoxynucleotidyl transferase reaction mix prepared according to the manufacturer's instructions for 60 min at 37 °C in a humidified chamber. The reaction was terminated with 2X SSC (15 min, room temperature), washed, and treated with 0.3% hydrogen peroxide to block endogenous peroxidases. Streptavidin horseradish peroxidase, hydrogen peroxide, and diaminobenzidine were then applied for 10 to 20 min at room temperature to identify apoptotic cells.

2.4 Nitric Oxide Response Assays

2.4.1 Diaphorase Staining—Diaphorase is a staining reaction that has been correlated with induction of NOS [31]. While diaphorase staining can occur for reasons unrelated to NO production, it is a less laborious and expensive procedure than immunochemical staining. It can also be applied after annexin V staining, enabling comparison of the two reactions in the same cultures. Fixed cells and washed explants were treated with diaphorase reaction solution containing NADPH (1.0 mg ml⁻¹), nitroblue tetrazolium (0.2 mg ml⁻¹), and 1.5% Triton X-100 in PBS (pH 7.4; [31] made just prior to use. The diaphorase reaction was carried out in the dark at 37 °C with agitation for 45–60 min.

2.4.2 uNOS Antibody staining—Rabbit anti-universal nitric oxide synthase (uNOS; Sigma-Aldrich), a commercially available antibody, was used to identify NOS. This antibody was made against the synthetic peptide to amino acids 1113-1122 of mouse iNOS and nNOS and recognizes all three mammalian NOS isoforms. This amino acid sequence also occurs in chicken iNOS [32], which made it a likely epitope for detecting NOS in turkey cells. Fixed cells were permeabilized by treating with 0.5% Triton X-100 in PBS for 15 min, washed twice in PBS (5 min), treated with 3% hydrogen peroxide, and again washed twice in PBS. Coverslips were then placed in a humidified chamber with the collagen gel-explant facing up and covered with 1/100 dilution of the antibody in 1% BSA/PBS, and incubated overnight at 4 °C. Immunohistological localization of NOS was accomplished using ExtrAvidin Peroxidase Staining Kit (Sigma-Aldrich) extending the incubation times of the secondary antibody to overnight and the extra-avidin step to 4 h, followed by staining using SIGMAFAST™ DAB (3,3'-Diaminobenzidine tetrahydrochloride) with Metal Enhancer staining solution (Sigma-Aldrich).

2.5 Microscopy

Videos of 197N treated cultures, cells washed from 197N treated cultures, and EBSS control cultures (videos 1, 2 and 3) were made using a video camera and video tape recorder mounted on an Olympus inverted phase contrast microscope and then converted to digital format. Annexin V staining was examined using a Nikon eclipse TE2000 inverted microscope, X-cite exfo epifluorescence light source, and Roper Scientific CoolSnap HQ monochrome digital camera. Nikon Elements software was used to capture 10 sec sequences of images and converted to AVI video format for display and analysis of the moving cilia (videos 3, 4, & 5). After washing, cultures that were stained for diaphorase, uNOS antibody, and TUNEL were covered with Crystal/Mount (Biomed), dried, and mounted in Permount (Fisher Scientific). Digital images of diaphorase, uNOS antibody, and TUNEL stained preparations were made using either a Zeiss microscope equipped with a Spot RT-slider cooled CCD imaging system (Diagnostics Instruments) or a Nikon Microphot microscope equipped with a Nikon DXM 1200F imaging system. For scanning electron microscopy, explant cultures were fixed with 2% glutaraldehyde, 2% paraformaldehyde, in 0.1 M cacodylate-HCl buffer, pH 7.4. After washing and dehydrating in an ethanol/acetone series, they were critically point dried (Polaron), sputter coated, and mounted on aluminum stubs. Specimens were examined and imaged using a Topcon ABT-32 Scanning Electron Microscope (SEM) with an Evex VidScan digital imaging system. For some images,

cropping, adjustment of contrast and brightness, and addition of scale bars were done using PaintShop Pro (Jasc Software).

3. Results

3.1 Active ciliated cells in explant cultures

After one to two days in explant culture, epithelial cells migrated from the edge of the explant toward the center or down the outside of the ring onto the surface of the collagen gel. After 3 to 4 days of incubation the edges of the epithelium met in the center, filling the central space (Fig. 1a). Many of these cells were ciliated (Fig. 1b, c) and the beating of the cilia was easily observed with phase contrast microscopy (videos 1) and differential interference contrast (DIC, videos 3). Active beating of the cilia continued for up to two weeks in these cultures. Extruded cells that were washed from the cultures (Fig. 1f) still showed weak ciliary movement (video 2).

3.2 The effect of *B. avium* on cilia behavior

Upon incubation with 10^8 *B. avium* cells ml^{-1} , the cultures exhibited a similar sequence of pathological changes as has been reported for *Bordetella* sp. both *in vivo* and for tracheal segments incubated with bacteria [2],[4–10], and [11]. By 24–36 h, ciliated cells were extruded from the epithelia (Figs. 1d, 1f, video 1) while cells in control cultures were normal in terms of both morphology and the behavior of the cilia observed in living and SEM cultures (Fig. 1c, video 1). In living cultures, the cilia of extruded cells (Fig. 1f) continued to show movement (video 2). The cilia of non-extruded cells were coated with bacteria, clumped together, and appeared to be unable to generate an effective power stroke (Fig. 1e, video 1). Within the first few hours of incubation, directed movement of particles had ceased although the cilia of infected cells continued to show movement.

3.3 Staining of tracheal cells by annexin V

The ciliated cells in cultures exposed to *B. avium* showed positive annexin V staining after 6 h of incubation (Fig. 2a, b, representative of eight experiments, and video 4). The positively staining cells (Fig. 2b) were not necrotic since their cilia showed normal morphology (Fig. 2a), were still moving (videos 3 & 4), and did not stain with PI (data not shown). Intact, non-ciliated epithelial cells did not show annexin V binding (Fig. 2b). In the EBSS treated controls there was a small subset of rounded, non-ciliated cells that stained positively although none of the actively beating ciliated cells (video 5) showed any annexin V staining (Fig. 2c, d, representative of eight experiments). Treatment with LPS, either $10 \mu\text{g ml}^{-1}$ *B. avium* LPS (Fig. 2 e,f) or 1, 10, or $100 \mu\text{g ml}^{-1}$ of *B. bronchiseptica* LPS (data not shown) also did not induce annexin V staining of ciliated cells. *B. bronchiseptica* LPS combined with TCT, and TCT alone did not induce annexin staining (data not shown). One experiment testing multiple explants for response to a mutant in the *wlb* operon affecting the terminal trisaccharide of *B. avium* LPS [33] was positive for annexin (data not shown, but identical to Fig. 2a and b), further supporting that LPS may not play a role in induction of apoptosis.

A supernatant fraction, treated so as to minimize dead and broken cells, was capable of inducing a positive annexin reaction (Fig. 2h) suggesting that molecules secreted by the bacteria into the medium may be responsible for inducing apoptosis. Boiling the supernatant before treatment abolished the annexin response (data not shown), suggesting a protein moiety was responsible. Further, a filtration procedure and subsequent testing narrowed the molecular weight of the toxic molecule to the range of 30 to 100 kDa. This positive induction of annexin staining (Fig. 2h) by bacteria-free culture media was observed in three experiments with unfractionated supernatant and three with fractionated supernatant. In three additional experiments, treatment of the cultures with *B. pertussis* Tohana 1 (Fig. 2i, j)

and two other *Bordetella* species (*B. bronchiseptica* RB50, and *B. hinzii* SV2, data not shown) produced no annexin staining over background levels.

3.4 Staining of tracheal cells by TUNEL

After incubation with *B. avium* 197n cells for 24 h, a larger proportion of tracheal cells showed a positive TUNEL reaction (Fig. 3a) than the EBSS controls (Fig. 3b). At 24 h both rounded-up ciliated and non-ciliated cells stained positive (Fig. 3c). The EBSS control samples contained few apoptotic cells (Fig. 3b), most of which were non-ciliated (Fig. 3d). EBSS cultures had mostly intact ciliated cells that showed no TUNEL staining (Fig. 3d). Images are representative of six experiments.

3.5 Staining of cilia by uNOS

Cultures continuously exposed to *B. avium* for 6 h or more showed positive immunohistochemical staining when a universal primary antibody for NOS was used (Fig. 4a, 4c, 5a). Only the cilia, and not the cell bodies, were stained by the antibody (Fig. 4c). Rounded, extruded cells, both ciliated and non-ciliated, also stained positively (data not shown). Ciliated epithelial cells in the EBSS controls did not stain (Fig. 4b, 4d). Cultures incubated with bacteria (Fig. 4e) or with EBSS (Fig. 4f) and treated with goat serum instead of anti-uNOS also did not stain.

Cultures treated with whole *B. avium* cells showed positive staining of cilia by both anti-uNOS (Fig. 5a) and by the diaphorase reaction (Fig. 5b). Treatment of explants cultures with *B. bronchiseptica* LPS (Fig. 5c) or *B. bronchiseptica* LPS with *B. pertussis* TCT (Fig. 5g) also showed some positive anti-uNOS staining of the cilia. LPS from *B. avium* was not available to test in these experiments; however, *B. avium* LPS is antigenically related to that of *B. bronchiseptica* and might be expected to produce the same reaction [24]. Furthermore, commercially available LPS from *Salmonella* produced identical induction of uNOS and staining for diaphorase (data not shown). Cells treated with TCT alone showed no anti-uNOS reactivity (Fig. 5e). The intensity and prevalence of the staining did not obviously change with simultaneous treatment of LPS and TCT (Fig. 5g) as compared to what was seen with LPS only (Fig. 5c). However, rigorous quantitation of the staining reaction has not been feasible. Images shown are representative of three experiments.

3.6 Induction of diaphorase by *B. avium* and other *Bordetellae*

The results for the diaphorase staining reaction are the same as for the anti-uNOS studies. Cultures that were continuously incubated with 10^8 *B. avium* ml⁻¹ for 6 h or longer showed diaphorase staining (Fig. 5b) while EBSS treated (control) cultures and cultures incubated for less than 6 h did not show any reaction (data not shown). Unlike the anti-uNOS staining, both ciliated and non-ciliated epithelial cells demonstrated a positive diaphorase reaction (Fig. 5b). In more intensely stained preparations, the cytoplasm of ciliated cells stained darkly, while in some lighter staining preparations only the cilia were stained. In non-ciliated cells the diaphorase staining was punctate and in the form of discrete cytoplasmic granules. Like they did with the anti-uNOS staining, LPS (Fig. 5d) and LPS with TCT (Fig. 5h) caused a clear diaphorase response while TCT alone showed only background staining (Fig. 5f). Images shown are representative of three experiments. Similar results were seen with commercially available LPS from *Salmonella typhimurium* (data not shown). In two additional experiments, treatment of the cultures with other *Bordetella* species (*B. pertussis* Tohama 1 (Fig. 6a), *B. bronchiseptica* RB50 (Fig. 6b), and *B. hinzii* (SV2) (Fig. 6c) produced similar staining patterns to *B. avium* 197N (Fig. 5b).

4. Discussion

In the trachea of infected birds, ciliated epithelial cells respond to *B. avium* attachment by rounding up, losing adhesion, and becoming extruded from the epithelium [3–6]. In the explanted organ culture developed for this study, ciliated tracheal cells responded in a similar fashion (Fig. 1). In these cultures, bacteria bound specifically to cilia, leading to the impairment of cilia activity and function, and eventual sloughing of ciliated cells from the collagen surface. These events were observed and recorded directly by DIC, phase contrast, fluorescent, and scanning electron microscopy (Fig. 1 and videos 1–5).

B. avium induced apoptosis in explant ciliated tracheal epithelium cells, as evidenced by cytochemical and immunochemical staining. Positive annexin V (Fig. 2) and TUNEL (Fig. 3) staining of ciliated cells treated with *B. avium* indicates the induction of proapoptotic events by the bacterium. A number of disorders and pathogens are known to initiate respiratory epithelial cell apoptosis resulting in aberrant host or pathogenic cell removal [12–13]. *Bordetellae* attachment to host cilia is extremely specific [5],[7], and [10–11]; thus selective elimination of ciliated cells via apoptosis would be beneficial to the host, resulting in the removal of the bacteria while maintaining epithelium barrier integrity.

In addition, *B. avium* triggered a strong NOS response in the ciliated tracheal cells, as shown by anti-uNOS (Fig. 4 & 5), and NADPH diaphorase (Fig. 5) staining. NO performs several roles in the respiratory system and the levels of NO present are controlled in two distinctive ways. Synthesis by constitutive nNOS and eNOS is controlled by calcium and the small quantities of NO produced act as intracellular messengers to control bronchial and vasomotor tone, mucus secretion, and ciliary activity [14],[16]. In contrast, increased expression of the iNOS gene results in larger quantities of NO that are toxic and initiate inflammation [14],[16]. iNOS has been reported in normal [34–35] and diseased [36] or endotoxin-treated respiratory epithelia [37]. Increased levels of eNOS staining have also been reported in diseased tissue [36],[38], but treatment with LPS increased epithelial staining for iNOS while decreasing eNOS staining [39]. The fact that it takes six hours for these reactions to appear after treatment with *B. avium*, rather than being instantaneous supports the idea that iNOS is being induced. However, since avian iNOS lacks the particular epitope used for commercially available forms of iNOS-specific antibodies [32], we were unable to directly determine whether increased staining is due to iNOS or simply the unmasking of one of the constitutive NOS forms found in respiratory cells.

Because we did not have *B. avium* LPS available at the time, first commercially prepared *Salmonella* LPS then *B. bronchiseptica* LPS were used in the LPS/TCT uNOS and diaphorase experiments. *B. bronchiseptica* LPS is antigenically related to that of *B. avium* [24] and produced results identical to those using the commercially available LPS from *Salmonella*. Turkey ciliated cells exposed to *B. bronchiseptica* and *Salmonella typhimurium* LPS alone stained positively for NOS and NADPH diaphorase activity, but neither they or *B. avium* LPS caused an annexin response. In *B. pertussis* infected hamster and human cells, TCT and LPS acted synergistically to induce pathological changes [15–18]. The action of these two virulence factors in *B. pertussis* was to induce NO production in adjoining non-ciliated cells and not in ciliated cells [17]. While the combination of TCT and LPS induces uNOS staining in avian cells, it did so only in the ciliated cells, and not in the adjacent non-ciliated cells (Fig. 5). TCT by itself had little effect on either the induction of uNOS staining (Fig. 5e), diaphorase staining (Fig. 5f) or annexin V staining in turkey tracheal cells. *B. avium* produces a TCT identical to one produced by *B. pertussis*, [26] but also has a functional AmpG permease (*ampG*) which recycles anhydromuropeptides like TCT back into the cell wall, thereby reducing the concentration of TCT present in the media. In *B. pertussis*, transcription of *ampG* is disrupted resulting in large quantities of TCT in culture

supernatants [24]. Thus TCT may not be present in sufficient concentration to have an impact on *B. avium* pathogenesis, and it appears that TCT by itself is not acting as a factor in inducing the *B. avium* apoptotic or the NOS response. In addition, the apoptotic response in *B. avium* is distinct from the NOS/diaphorase response since *B. avium* LPS was able to induce NOS and diaphorase, but did not initiate an apoptotic (annexin V) reaction. Other *Bordetella* species (*B. pertussis*, *B. bronchiseptica*, *B. hinzii*), and *Salmonella typhimurium* LPS also induced diaphorase staining indicating activation of the NO pathway (Fig. 6) but not annexin staining (Fig. 2j, and data not shown). Thus, it appears that the two responses are being initiated by different factors in *B. avium*. Since uNOS and diaphorase staining can be induced by LPS from different *Bordetella* species, it appears that induction of the NO pathway in turkey tracheal cells is not species specific, indicating that it is due (at least in part) to conserved LPS components, since LPS among the *Bordetella* varies [40–41]

Although both *Bordetella* species cause diseases with similar characteristics, these studies indicate that the pathogenesis of *B. avium* is influenced by different bacterial factors than those found in *B. pertussis*. This supports our previous genomic comparison studies that found *B. avium* to lack several of the virulence-associated toxins of *B. pertussis* [24]. The novel explant organ culture system allowed study of the response of the natural host to *B. avium* and will be used in future experiments to further understand the events of pathogenesis [33] and identify the bacterial factors that are responsible. Future studies involving the further purification of *B. avium* supernatant factors that induce apoptosis in turkey tracheal explants constitute the next critical steps in the discovery of these unknown virulence factors. Elimination of identified toxin genes in attachment proficient bacteria could be the basis for a live, attenuated vaccine strain.

Supplementary Material

Refer to Web version on PubMed Central for supplementary material.

Acknowledgments

This work was supported by College of Liberal Arts, Drew University Funding to LMT and DMM, and an NIH grant R15A157382-01 to LMT and DMM.

References

1. Temple LM, Weiss AA, Walker KE, Barnes HJ, Christensen VL, Miyamoto DM, Shelton CB, Orndorff PE. *Bordetella avium* virulence measured in vivo and in vitro. *Infect. Immun.* 1998; 66:5244–5251. [PubMed: 9784529]
2. Saif YM, Moorhead PD, Whitmoyer RE. Scanning electron microscopy of tracheas from turkey poultts infected with *Alcaligenes faecalis*. *Avian Dis.* 1981; 25:730–735. [PubMed: 7316906]
3. Arp LH, Cheville NF. Tracheal lesions in young turkeys infected with *Bordetella avium*. *Am. J. Vet. Res.* 1984; 45:2196–2200. [PubMed: 6497122]
4. Arp LH, Fagerland JA. Ultrastructural pathology of *Bordetella avium* infection in turkeys. *Vet. Pathol.* 1987; 24:411–418. [PubMed: 3672806]
5. Gray JG, Roberts JF, Dillman RC, Simmons DG. Cytotoxic activity of pathogenic *Alcaligenes faecalis* in turkey tracheal organ cultures. *Am. J. Vet. Res.* 1981; 42:2184–2186. [PubMed: 7340589]
6. Gray JG, Roberts JF, Dillman RC, Simmons DG. Pathogenesis of change in the upper respiratory tracts of turkeys experimentally infected with an *Alcaligenes faecalis* isolate. *Infect. Immun.* 1983; 42:350–355. [PubMed: 6618668]
7. Sekiya K, Futaesaku Y, Nakase Y. Electron microscopic observations on tracheal epithelia of mice infected with *Bordetella bronchiseptica*. *Microbiol. Immunol.* 1988; 32:461–472. [PubMed: 3173144]

8. Collier AM, Peterson LP, Baseman JB. Pathogenesis of infection with *Bordetella pertussis* in hamster tracheal organ culture. *J. Infect. Dis.* 1977; 136 Suppl:S196–S203. [PubMed: 197174]
9. Muse KE, Collier AM, Baseman JB. Scanning electron microscopic study of hamster tracheal organ cultures infected with *Bordetella pertussis*. *J. Infect. Dis.* 1977; 136:768–777. [PubMed: 200679]
10. Soane MC, Jackson A, Maskell D, Allen A, Keig P, Dewar A, Dougan G, Wilson R. Interaction of *Bordetella pertussis* with human respiratory mucosa in vitro. *Respir. Med.* 2000; 94:791–799. [PubMed: 10955756]
11. Opremcak LB, Rheins MS. Scanning electron microscopy of mouse ciliated oviduct and tracheal epithelium infected in vitro with *Bordetella pertussis*. *Can. J. Microbiol.* 1983; 29:415–420. [PubMed: 6850422]
12. Tesfaigzi Y. Roles of apoptosis in airway epithelia. *Am. J. Respir. Cell Mol. Biol.* 2006; 34:537–547. [PubMed: 16439804]
13. Weinrauch Y, Zychlinsky A. The induction of apoptosis by bacterial pathogens. *Annu. Rev. Microbiol.* 1999; 53:155–187. [PubMed: 10547689]
14. Ricciardolo FL. Multiple roles of nitric oxide in the airways. *Thorax.* 2003; 58:175–182. [PubMed: 12554905]
15. Heiss LN, Flak TA, Lancaster JR Jr, McDaniel ML, Goldman WE. Nitric oxide mediates *Bordetella pertussis* tracheal cytotoxin damage to the respiratory epithelium. *Infect. Agents Dis.* 1993; 2:173–177. [PubMed: 8173789]
16. Flak TA, Goldman WE. Autotoxicity of nitric oxide in airway disease. *Am. J. Respir. Crit. Care Med.* 1996; 154:S202–S206. [PubMed: 8876543]
17. Flak TA, Goldman WE. Signalling and cellular specificity of airway nitric oxide production in pertussis. *Cell. Microbiol.* 1999; 1:51–60. [PubMed: 11207540]
18. Flak TA, Heiss LN, Engle JT, Goldman WE. Synergistic epithelial responses to endotoxin and a naturally occurring muramyl peptide. *Infect. Immun.* 2000; 68:1235–1242. [PubMed: 10678932]
19. Canthaboo C, Xing D, Wei XQ, Corbel MJ. Investigation of role of nitric oxide in protection from *Bordetella pertussis* respiratory challenge. *Infect. Immun.* 2002; 70:679–684. [PubMed: 11796599]
20. Banan A, Fields JZ, Decker H, Zhang Y, Keshavarzian A. Nitric oxide and its metabolites mediate ethanol-induced microtubule disruption and intestinal barrier dysfunction. *J. Pharmacol. Exp. Ther.* 2000; 294:997–1008. [PubMed: 10945852]
21. Brune B. Nitric oxide: NO apoptosis or turning it ON? *Cell Death Differ.* 2003; 10:864–869. [PubMed: 12867993]
22. Monteiro HP, Silva EF, Stern A. Nitric oxide: a potential inducer of adhesion-related apoptosis--anoikis. *Nitric Oxide.* 2004; 10:1–10. [PubMed: 15050529]
23. Stout SL, Wyatt TA, Adams JJ, Sisson JH. Nitric oxide-dependent cilia regulatory enzyme localization in bovine bronchial epithelial cells. *J. Histochem. Cytochem.* 2007; 55:433–442. [PubMed: 17242464]
24. Sebahia M, Preston A, Maskell DJ, Kuzmiak H, Connell TD, King ND, Orndorff PE, Miyamoto DM, Thomson NR, Harris D, Goble A, Lord A, Murphy L, Quail MA, Rutter S, Squares R, Squares S, Woodward J, Parkhill J, Temple LM. Comparison of the genome sequence of the poultry pathogen *Bordetella avium* with those of *B. bronchiseptica*, *B. pertussis*, and *B. parapertussis* reveals extensive diversity in surface structures associated with host interaction. *J. Bacteriol.* 2006; 188:6002–6015. [PubMed: 16885469]
25. Di Fabio JL, Caroff M, Karibian D, Richards JC, Perry MB. Characterization of the common antigenic lipopolysaccharide O-chains produced by *Bordetella bronchiseptica* and *Bordetella parapertussis*. *FEMS Microbiol. Lett.* 1992; 76:275–281. [PubMed: 1427018]
26. Gentry-Weeks CR, Cookson BT, Goldman WE, Rimler RB, Porter SB, Curtiss R 3rd. Dermonecrotic toxin and tracheal cytotoxin, putative virulence factors of *Bordetella avium*. *Infect. Immun.* 1988; 56:1698–1707. [PubMed: 3384473]
27. Connell TD, Dickenson A, Martone AJ, Militello KT, Filiatraut MJ, Hayman ML, Pitula J. Iron starvation of *Bordetella avium* stimulates expression of five outer membrane proteins and regulates a gene involved in acquiring iron from serum. *Infect. Immun.* 1998; 66:3597–3605. [PubMed: 9673238]

28. Van Engeland M, Nieland LJW, Ramaekers FCS, Schutte B, Reutelingsperger CPM. Annexin V-affinity assay: A review on an apoptosis detection system based on phosphatidylserine exposure. *Cytometry*. 1998; 31:1–9. [PubMed: 9450519]
29. Koopman G, Reutelingsperger CPM, Kuijten GAM, Keehnen RMJ, Pals ST, Van Oers MHJ. Annexin V for flow cytometric detection of phosphatidylserine expression on B cells undergoing apoptosis. *Blood*. 1994; 84:1415–1420. [PubMed: 8068938]
30. Gavrieli Y, Sherman Y, Ben-Sasson SA. Identification of programmed cell death in situ via specific labeling of nuclear DNA fragmentation. *J. Cell Biol.* 1992; 119:493–501. [PubMed: 1400587]
31. Lee SH, Iwanaga T, Hoshi O, Adachi I, Fujita T. Nitric oxide synthase in rat nasal mucosa; immunohistochemical and histochemical localization. *Acta Otolaryngol.* 1995; 115:823–829. [PubMed: 8749206]
32. Lin AW, Chang CC, McCormick CC. Molecular cloning and expression of an avian macrophage nitric-oxide synthase cDNA and the analysis of the genomic 5'-flanking region. *J. Biol. Chem.* 1996; 271:11911–11919. [PubMed: 8662618]
33. Spears PA, Temple LM, Miyamoto DM, Maskell DJ, Orndorff PE. Unexpected similarities between *Bordetella avium* and other pathogenic bordetellae. *Infect. Immun.* 2003; 71:2591–2597. [PubMed: 12704133]
34. Kobzik L, Brecht DS, Lowenstein CJ, Drazen J, Gaston B, Sugarbaker D, Stamler JS. Nitric oxide synthase in human and rat lung: immunocytochemical and histochemical localization. *Am. J. Respir. Cell Mol. Biol.* 1993; 9:371–377. [PubMed: 7691109]
35. Rosbe KW, Mims JW, Prazma J, Petrusz P, Rose A, Drake AF. Immunohistochemical localization of nitric oxide synthase activity in upper respiratory epithelium. *Laryngoscope.* 1996; 106:1075–1079. [PubMed: 8822708]
36. Kawamoto H, Takumida M, Takeno S, Watanabe H, Fukushima N, Yajin K. Localization of nitric oxide synthase in human nasal mucosa with nasal allergy. *Acta Otolaryngol. Suppl.* 1998; 539:65–70. [PubMed: 10095865]
37. Buttery LD, Evans TJ, Springall DR, Carpenter A, Cohen J, Polak JM. Immunohistochemical localization of inducible nitric oxide synthase in endotoxin-treated rats. *Lab. Invest.* 1994; 71:755–764. [PubMed: 7526041]
38. Furukawa K, Harrison DG, Saleh D, Shennib H, Chagnon FP, Giaid A. Expression of nitric oxide synthase in the human nasal mucosa. *Am. J. Respir. Crit. Care Med.* 1996; 153:847–850. [PubMed: 8564142]
39. Ermert M, Ruppert C, Gunther A, Duncker HR, Seeger W, Ermert L. Cell-specific nitric oxide synthase-isoenzyme expression and regulation in response to endotoxin in intact rat lungs. *Lab. Invest.* 2002; 82:425–441. [PubMed: 11950900]
40. Preston A, Petersen BO, Duus JO, Kubler-Kielb J, Ben-Menachem G, Li J, Vinogradov E. Complete structures of *Bordetella bronchiseptica* and *Bordetella parapertussis* lipopolysaccharides. *J. Biol. Chem.* 2006; 281:18135–18144. [PubMed: 16632471]
41. Preston A, Mandrell RE, Gibson BW, Apicella MA. The lipooligosaccharides of pathogenic gram-negative bacteria. *Crit. Rev. Microbiol.* 1996; 22:139–180. [PubMed: 8894399]

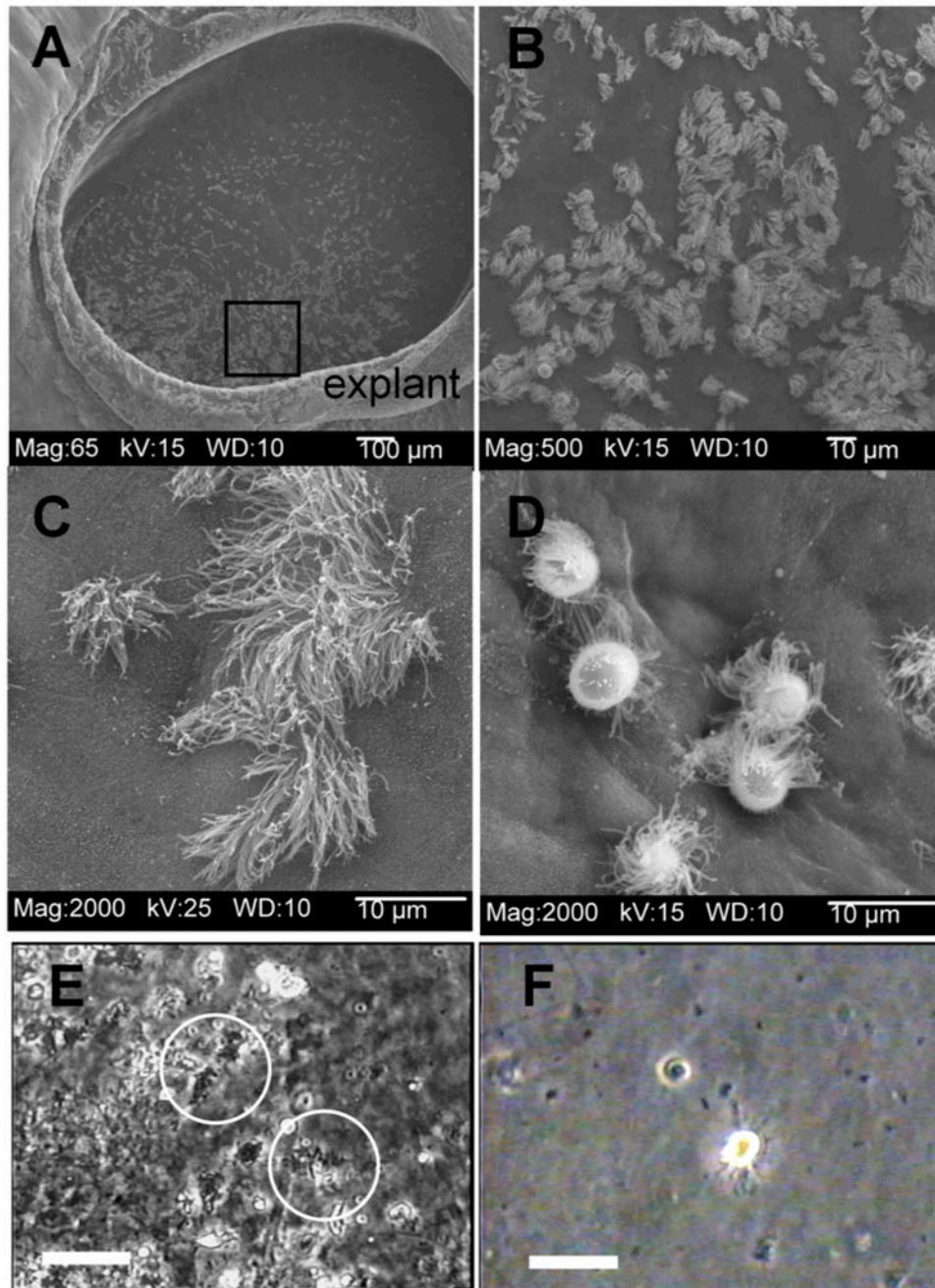


Figure 1. Response of explant cultures of turkey trachea to *B. avium*

Scanning Electron Micrograph of Tracheal ring explant, 4 d incubation, showing the migration of the epithelium into and filling the center (Fig. 1a). The area shown by the box (Fig. 1a) is seen at higher magnification in Fig. 1b, which shows ciliated and non-ciliated epithelia cells. Healthy ciliated cells are still present after 32h of incubation in EBSS (Fig. 1c) while incubation with 10^8 *B. avium* 197n cells for 32 h shows extruded ciliated cells on the surface of non-ciliated epithelial cells (Fig. 1d). Figure 1e shows a frame captured from a phase contrast video recording of a culture treated with 10^8 *B. avium* 197n after 22 h of incubation. In the video, ciliated cells (circles) have numerous bacteria attached to their cilia and a disrupted beating of the cilia (video 1). Figure 1f shows a frame captured from the

video recording of extruded ciliated cells washed from the explant culture 24 hours after the start of incubation in order to see clearly the movements of cilia still occurring (video 2). Scale bars for Fig. 1e and 1f = 20 μm .

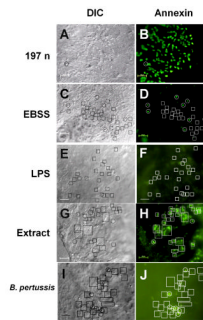


Figure 2. Annexin V staining of explant culture cells

Cultures were incubated with 197N *B. avium* (10^8 cells ml^{-1} , Fig. 2a, b), EBSS (Fig. 2c, d), *B. avium* LPS (Fig. 2e, f), 10^{-1} dilution of a cell free supernatant (Fig. 2g, h) or *B. pertussis* Tohama 1 (10^8 cells ml^{-1} , Fig. 2i, j), for 6 h and stained with annexin V Alexa Fluor 488. Fig. 2a, c, e, g, & i are DIC images of the same field as the fluorescence images of the annexin V staining (Fig. 2b, d, f, h, & j). In these examples 10–20 s video sequences of the movement of the cilia were also recorded, confirming that the fluorescence was associated with the cilia (videos 3, 4, & 5). Comparing the fluorescence image (Fig. 2b) with the DIC image (Fig. 2a) and video sequence (videos 3 & 4) showed all of the ciliated cells in cultures treated with 197n had positively stained with annexin V. Areas where there were no ciliated cells had no discernable fluorescence, demonstrating that non-ciliated epithelial cells did not have an immediate annexin response to the presence of bacteria. In the EBSS treated cultures the cells that showed positive staining (white circles, Fig. 2d) were round, non-ciliated cells in the DIC image (black circles, Fig. 2c). Actively beating ciliated cells (black boxes, Fig. 2c, video 5) showed no annexin staining (white boxes, Fig. 2d). *B. avium* LPS also failed to induce annexin staining of ciliated cells, as again the active cilia (black boxes, Fig. 3e) showed no fluorescence (white boxes, Fig. 3f). A 1/10 dilution of bacteria free media did induce annexin staining (Fig. 2h, white boxes) of active ciliated cells (Fig. 3g, boxes). Treatment with *B. pertussis* also did not cause an annexin response (Fig. 2j, black boxes) in active ciliated cells (Fig. 2i, boxes). Scale bars= 50 μm .

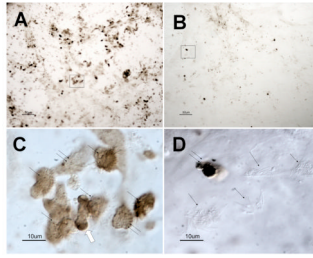


Figure 3. TUNEL staining of explant cultures treated with *B. avium* 197n and EBSS
B. avium 197n (Fig. 3a, 3c) and EBSS (Fig. 3b, 3d) treated explants after 24 h of incubation. Fig. 3a and 3b are low magnification bright field images showing the greater amount of TUNEL staining of the 197n treated cultures. The positively staining cells in Fig. 3a (boxed area) are rounded ciliated (single arrow) and non-ciliated (double arrows) when viewed at higher magnification with DIC (Fig. 3c). It appears that the cells are fragmenting with TUNEL positive material being extruded (large arrow, Fig. 3c). Positively stained cells in the EBSS treated cultures (boxed area, Fig. 3b) were typically non-ciliated cells (Fig. 3d, double arrows) surrounded by intact ciliated cells (Fig. 3d, single arrows). Scale bars for Fig. 3a and b= 50 μ m. Scale bars for Fig. 3c and 3d= 10 μ m.

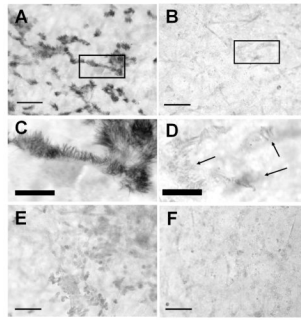


Figure 4. Immunohistochemical staining for uNOS, bright field microscopy

Tracheal ring cultures, fixed and stained 6 h following initial treatment. Cultures continuously exposed to 10^8 *B. avium* cells ml^{-1} *B. avium* for 6–8 h showed positive immuno-histochemical staining when a primary antibody for all three isoforms of NOS was used (Fig. 4a). Control cultures incubated without bacteria and treated with anti-uNOS did not stain (Fig. 4b). Closer examination (boxes, Fig. 4a, 4b) indicated that only the cilia showed positive anti-uNOS staining (Fig. 4c) in bacteria treated cultures. Cilia in the EBSS control (arrows) did not stain (Fig. 4d). Cultures incubated with bacteria (Fig. 4e) or EBSS (Fig. 4f) and treated with goat serum rather than anti-uNOS showed no positive antibody staining. Fig. 4a, b, e, f are all the same magnification, bar in lower left corner = 50 μm . Fig. 4c, d are the same magnification, bar = 20 μm .

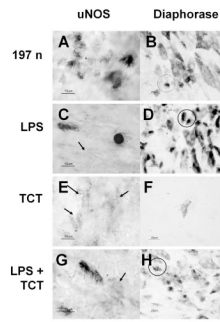


Figure 5. uNOS and diaphorase staining of cultures treated with LPS and TCT

Brightfield microscopy of tracheal ring cultures after 24 h of incubation. Fig. 5a, 5c, 5e, 5g = cultures stained by anti-uNOS immunostaining. Fig. 5b, 5d, 5f, 5h = diaphorase staining. Circles designate stained ciliated cells, while arrows designate unstained ciliated cells. Scale bars in lower left corners. Fig. 5a, 5b= tracheal explants treated with whole cell 197n bacteria. Fig. 5c, 5d= tracheal explants treated with 1 mg ml^{-1} purified *Bordetella bronchiseptica* LPS. Fig. 5e, 5f= tracheal explants treated with 1 M purified *Bordetella pertussis* TCT. Fig. 5g, 5h= tracheal explants treated with *B. bronchiseptica* LPS and *B. pertussis* TCT. Not shown: EBSS treated explants cultures that were negative for anti-uNOS or diaphorase staining. LPS treatment shows both non-extruded and extruded ciliated cells staining for uNOS while other intact ciliated cells did not show a reaction (Fig. 5c, arrow). LPS and TCT together (Fig. 5g & 5h) produced similar results as LPS alone (Fig. 5c & 5d). TCT by itself did not induce either anti-uNOS or diaphorase staining (Fig. 5e & 5f).

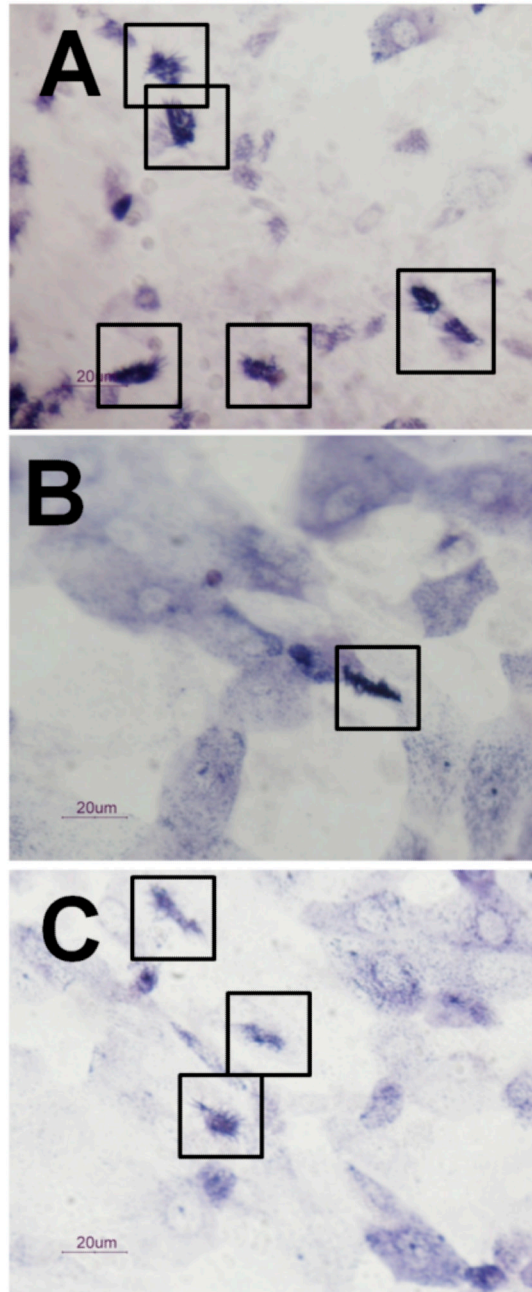


Figure 6. Reaction of turkey tracheal epithelia cells to other *Bordetella* species

Diaphorase staining of turkey tracheal epithelial cells treated with *B. pertussis* Tohama 1 (Fig. 6a), *B. bronchiseptica* RB50 (Fig. 6b,) and *B. hinzei* (SV2) (Fig. 6c) after being first being stained for annexin. All of these cultures showed a negative annexin response (Fig. 2i, j, data not shown), but show diaphorase staining of ciliated (boxes) and non-ciliated cells similar to what is observed in *B. avium* 197n (Fig. 5b). Scale bars= 20µm.